Stochastic-Deterministic Electromagnetic Modeling of Human Head Exposure to Microsoft HoloLens

Ante Lojić Kapetanović*, Anna Šušnjara† Dragan Poljak‡, Mladen Russo§
Faculty of Electrical Engineering, Mechanical Engineering and Naval Architecture
University of Split
Split, Croatia
*alojic00@fesb.hr, †asusnja@fesb.hr, ‡dpoljak@fesb.hr, §mrusso@fesb.hr

***Abstract*—In this paper, the electromagnetic (EM) simulation of the exposure of a spherical model of the human head to the HoloLens, a mixed reality device developed and manufactured by Microsoft, is performed at 10 GHz in addition to IEEE 802.11ac Wi-Fi frequencies of 2.4 and 5 GHz. The compliance assessment with current guidelines and standards for limiting human exposure to EM fields up to 300 GHz by means of incident power density (IPD) is provided at separation distances between the model and antenna ranging from 2.5 to 150 mm. The effect of the curvature of the average adult and child head on the IPD is investigated on a control surface of 4 cm^2. Results stemming from stochastic analysis indicate marginal difference between the spatially averaged IPD on the two distinct head models. On the other hand, comparative analysis of the spatially averaged IPD on the least and most curved body parts points to relative differences of up to 20% in certain exposure scenarios. Overall, spherical head models yield significantly higher values of the spatially averaged IPD (up to 25%) compared to standard planar models. It is therefore important to consider the inherent curvature of the nonplanar exposed body parts (e.g., head) to accurately assess targeted exposure quantities.**

***Index Terms*—electromagnetic simulation, exposure assessment, incident power density, human head, Microsoft HoloLens**

I. Introduction

Recent advances in wireless communication gave rise to the fifth-generation (5G) technology standard for broadband cellular networks. The most notable performance features are reflected through reduced latency, improved error rate and data transfer speed (carrier aggregation, massive multiple-input and multiple-output (MIMO) technology, beamforming, etc.) [1]. Expansion of the frequency spectrum compared to preceding generations led to increased channel capacity at the expense of signal coverage area – ideal for urban areas with a large amount of data-intensive devices [2]. One such device is the Microsoft HoloLens, a mixed reality headset with transparent lenses. Mixed reality technology with its immersive and augmentative features enables numerous real-life applications. One of the first and most important applications is in the healthcare, where it can enable technologically advanced diagnosis, training, planning and implementation of examinations and surgical procedures. Microsoft HoloLens and other mixed and augmented reality devices are head mounted devices (HMDs) and, regarding the medical applications and procedures, are required to be worn for a longer periods of time. In such uses and circumstances, exposure of the human head to EM fields has to be accounted and analyzed. HoloLens supports two methods for wireless network communication: an *ad hoc* IEEE 802.11ac Wi-Fi at 2.4 and 5 GHz, and 5G via USB-C connected dongle [3].

In order to ensure safety and to limit exposure to EM fields up to 300 GHz, both international guidelines by ICNIRP [4] and standards by IEEE [5] have been revisited fairly recently as a response to the massive deployment of 5G base station antennas and hand-held or body-worn devices. At frequencies below 6 GHz, specific absorption rate is used as the basic restriction, while above this transition frequency, the absorbed [4] or epithelial power density [5] is instead used to take into account the dominant heating effect of superficial exposed tissues [6]. To alleviate the issue of internal dosimetric measuring of exposed tissue, reference levels are derived from the basic restrictions to provide a practical means of demonstrating compliance to guidelines and standards. Reference levels for local exposure to EM fields from 100 kHz to 300 GHz are typically averaged over 6 minutes and are expressed by means of the IPD either through its peak value (from 2 to 6 GHz) or the spatially averaged value (at and above 6 up to 300 GHz). Spatial averaging is performed on a square evaluation plane of 4 cm^2 area to ensure consistency with volumetric averaging at lower frequencies [7]. To account for narrow beam formation at higher frequencies, averaging above 30 GHz should additionally be performed on a square 1 cm^2 area, provided it results in at most twice the value of 4 cm^2 area [8].

The IPD correlates strongly (Pearson correlation coefficient > 0.7 according to [9]) with basic restrictions, and, in turn, with superficial temperature rise, in the radiative near-field and far-field zone [10]–[12]. Within the reactive near-field zone (separation distance $<$ wavelenght$/2\pi$ from the antenna), the reference values are treated as inadequate and the compliance should be provided by assessing basic restrictions instead [13]. However, most of the relevant dosimetric studies use either planar single- or multi-layer block tissue-equivalent models which can result in rather poor estimation of the exposure level if the nonplanar geometry of the exposed tissue is pronounced,

This research has been supported by the Virtual Telemedicine Assistance - VITA, a project co-financed by the Croatian Government and the European Union through the European Regional Development Fund - the Competitiveness and Cohesion Operational Programme (KK.01.1.1.01).

e.g., the wavelength of incident fields is of the same order of magnitude as the radius of the curved body part [14].

In this study, we first investigate the effect of the curvature of the human head on the spatially averaged IPD. Two head models are considered: the adult and child head model of average dimensions. Stochastic analysis of the influence of uncertainty of curvature is also performed. Moreover, we analyze the difference between the spatially averaged IPD on small, curved body parts and flat body parts. The paper is outlined as follows. Section II introduces exposure scenarios and formulates the expression for the assessment of the spatially averaged IPD. Computational results and discussion are provided in Sec. III. Finally, concluding remarks and some future research directions can be found in Sec. IV.

II. Materials and Methods

A. Exposure Scenario

The 2-by-2 MIMO antenna is fixed in the posterior pad of the HoloLens. It features IEEE 802.11ac Wi-Fi supported by the SDM850 chipset where the connectivity is achieved at 2.4 and 5 GHz [15]. In this work, we also consider 5G network connection at 10 GHz via tethered dongle to account for the compliance with the current guidelines [4] and standards [5] above 6 GHz. For simplicity sake, the antenna is modeled as a half-wavelength dipole driven by a voltage source set to 1 V. The current distribution over thin wire (radius of the antenna is set to 1/10 of the antenna length) is governed by the Pocklington equation [16] and the solution is carried out by using in-house code based on the indirect boundary element method [17]. Electric and magnetic field components are computed at points on the surface of the exposed tissue assuming free space conditions by using integral expressions as given in [17]. Separation distances between the antenna and the model are set in 2.5 to 150 mm range given the possibility of adjustment of the placement of the rear pad within which the antenna is installed.

Since the antenna is placed nearby the most curved region of the head, the curvature of the control surface had to be taken into account when computing the spatially averaged IPD. The curvature is approximated by using a spherical model and is controlled by changing the associated radius. Two cases are considered in the study: the average male adult head model with a radius of 15.2 cm (the average vertical distance from the nasal root depression between the eyes to the level of the top of the head [18]), Fig. 1(a), and the average five-year-old child head model with a radius of 11.4 cm (derived from the WHO child growth standards [19]), Fig. 1(b). The position between the antenna and the general control surface on the head model is shown in Fig. 1(c).

In addition, the effect of the curvature of small parts on the human head (e.g. ear helix, eye, etc.) is also examined and inter-compared with the parietal head region. Two edge cases are considered: the minimal radius, r_{min}, of 1.8 cm, which is the smallest radius to allow spatial averaging of the incident power density on 4 cm^2 control area, and the maximal radius, r_{max}, arbitrarily set to $10 \times r_{\text{min}}$. The ratio of control surfaces corresponding to radii of 1.8 and 18 cm is shown in Fig. 2.

B. Assessment of the Incident Power Density

The spatially averaged IPD is represented as the surface integral of the normal component of the time-averaged Poynting vector in free space across the control surface of area, A, and is given as follows [9]

$$sPD = \frac{1}{A} \iint_A \frac{1}{2} \, \Re\big[\boldsymbol{E} \times \boldsymbol{H}^*\big] \, \boldsymbol{n} \, \mathrm{d}A \tag{1}$$

where $\boldsymbol{E}$ and $\boldsymbol{H}^*$ are peak values of the electric and complex-conjugate magnetic field, respectively, $\boldsymbol{n}$ is the unit vector normal to the control surface, and $\mathrm{d}A$ is the differential area element. Spatial distribution of the unit vector normal to A is computed in spherical coordinate system by following the approach proposed in [20] and is shown on a 4 cm^2 control surface in Fig. 1(c). Although the spatial averaging applies only to frequencies at and above 6 GHz, the analysis performed in subsequent section takes averaging rather than peak values into account at lower frequencies as well. This is primarily so that the curvature would have an impact where in the case of the peak value definition, the IPD in the same point in space, regardless of whether a curved or planar model is utilized, would be computed (the planar model is represented as a tangential surface at the point on the curved model closest to the antenna).

C. Uncertainty Quantification

Stochastic collocation (SC) is used as the method of choice for the propagation of uncertainties of input curvature to the output IPD. SC is a powerful tool in stochastic dosimetry because of its inherent non-intrusive nature which allows the use of deterministic models as is. By relying on the polynomial representation of the stochastic output, the number of simulations is significantly reduced compared to traditional methods, e.g., Monte Carlo [21].

sPD, computed by using (1), is approximated by its surrogate constructed as follows

$$\widetilde{sPD} = \sum_{k=1}^{n} L_k(r) \cdot sPD_k \tag{2}$$

where sPD_k is the value of the IPD from the k-th deterministic computation, $k = 1, 2, \ldots, n$, r denotes the curvature which is represented as the uniformly distributed random variable, and L_k is the k-th basis function of Lagrange type.

From (2), the first two statistical moments of interest are derived: mean, $\mu(sPD; r)$, defined as

$$\mu(sPD; r) \approx \sum_{k=1}^{n} sPD_k \cdot w_k \tag{3}$$

and variance, $\sigma^2(sPD; r)$, a measure of dispersion defined as

$$\sigma^2(sPD; r) \approx \sum_{k=1}^{n} sPD_k^2 \cdot w_k - [\mu(sPD; r)]^2 \tag{4}$$

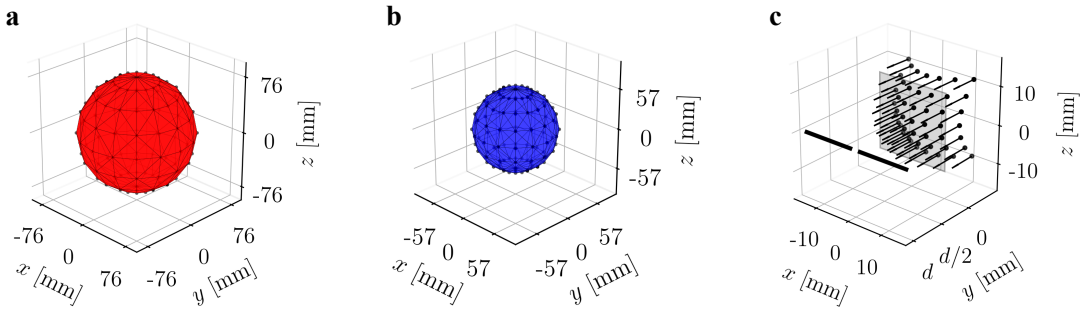

Fig. 1. Spherical head models used for the EM exposure assessment: (a) average adult male, (b) five-year-old male child, (c) evaluation points on the curved control surface in which the IPD is computed, black dashed line represents the position of the dipole antenna, gray plane represents the planar control surface used as a reference, and full black lines represent the spatial distribution of the unit vector normal to the surface.

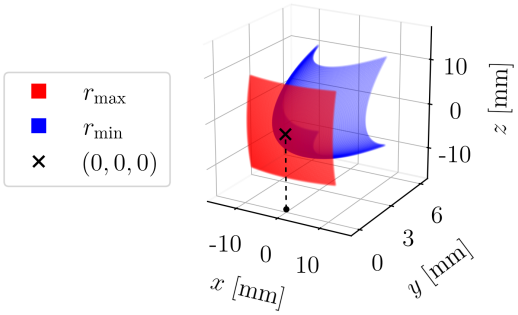

Fig. 2. Positional relationship of 4 cm^2 control surfaces spherical in shape corresponding to the radii of $r_{\min} = 1.8$ cm and $r_{\max} = 18$ cm.

In (3) and (4), the weight of the k-th input point is computed as

$$w_k = \int_{r_a}^{r_b} L_k(r) \cdot pdf(r)\, \mathrm{d}r \tag{5}$$

where $pdf(r)$ is the probability density function of r — in this case, represented as the uniform distribution within boundaries $(r_a,\ r_b)$.

III. Computational Results and Discussion

A. Stochastic Analysis of Incident Power Density on Human Head

In order to consider the variability of human head anatomy, a stochastic analysis of the influence of curvature on the spatially averaged IPD has been performed. By using the SC method with 7 collocation points, the uncertainty of spatially averaged IPD on both the adult and child head model is determined and placed inside the 99 % confidence interval. Spherical models' radii are set as random variables uniformly distributed inside the open bounds limited by the minimum and maximum value respectively derived as expected values $\pm$ 3 standard deviations. For the case of the adult head model, the bounds are (13.52 cm, 16.88 cm) and for the case of the child head model, the bounds correspond to (10.14 cm, 12.66 cm).

Results comparing sPD averaged on a control surface of the adult head model, the child head model, and the planar model as a function of the separation distance from the antenna, d, are shown in the first row in Fig. 3. It is obvious that sPD decreases rather monotonically with an increase in separation distance and finally reaches about 0.025 W m^{-2} at $d = 150$ mm at all considered frequencies. The highest mean value of 8.40 W m^{-2} is captured at $f = 10$ GHz and $d = 2.5$ mm on the child head model. It is important to notice that variations in radii for both head models do not contribute to significant variations of the spatially averaged IPD. The largest standard deviation of 4.23×10^{-2} W m^{-2} is captured at $f = 10$ GHz and $d = 2.5$ mm on the child head model. Overall, the child head model yields highest values of both the mean sPD and standard deviation for all considered cases with larger differences observed at shorter separation distances. Since the uncertainty of the output is negligible, further analysis is provided only by considering mean values.

The relative percentage difference in sPD is calculated as follows

$$\%\ \text{difference} = \frac{\Delta sPD}{sPD_{\text{ref}}} \cdot 100 \tag{6}$$

where ΔsPD is the difference between compared mean sPD values, and sPD_{ref} represents the corresponding value computed on an evaluation plane and is used as the reference. Largest relative differences are captured at shorter separations distances, but by increasing d, relative differences decrease and end up within $\pm$ 1 % for all cases at $d \geq 50$ mm. Relative differences between the adult and child head model are low regardless of d at all frequencies which further verifies the lack of the effect that variations of curvature have on sPD. However, by comparing sPD on the adult head model and a planar surface, and on the child head model and a planar surface, relative differences are shown to be significant at short separation distances. The largest relative difference in sPD between the adult head model and a planar surface is 11.33 % and between the child head model and a planar surface is 8.82 %, in both cases at $f = 5$ GHz and $d = 2.5$ mm. This indicates that even though small variations in radii of curved models do not have a substantial effect on overall sPD, the

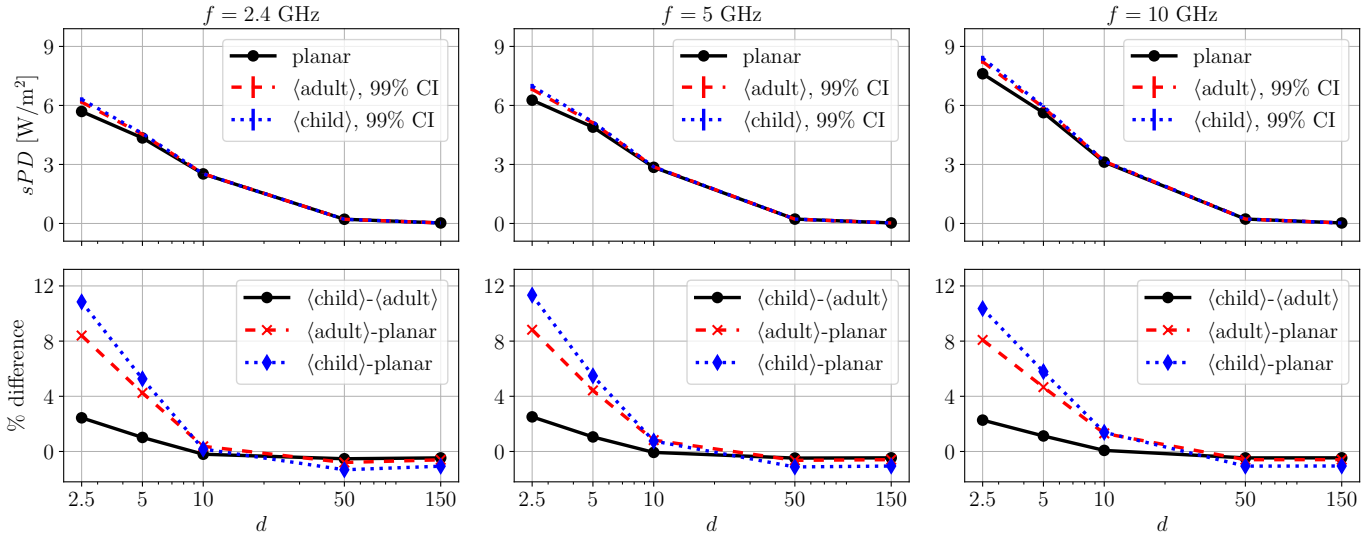

Fig. 3. The first row shows sPD averaged on an evaluation plane (used as a reference) and on the adult and child head models as a function of the separation distance from the antenna at 2.4 GHz, 5 GHz and 10 GHz. The second row shows relative differences in sPD between two head models and between each head model and its planar counterpart.

curvature itself does play a significant role especially in near field.

B. Deterministic Analysis of Incident Power Density on Small Spherical Body Parts

In this subsection, small nonplanar parts of the human head, e.g., human eye, ear, or skull deformities, are approximated with the spherical model with the radius, r_{min}, set to 1.8 cm. sPD on small nonplanar body parts are compared with sPD averaged on only slightly curved region of the human head, e.g., partiel region, which is approximated with the spherical model where the radius, r_{max}, is set to 18 cm. For the simplicity sake, the model with the radius r_{max} is referred to as "max" while the model with the radius set to r_{min} is referred to as "min". On both models, sPD decreases with an increase in d up to $d = 50\,\text{mm}$. At $d = 50\,\text{mm}$, sPD is slightly lower than sPD at $d = 150\,\text{mm}$ where it finally reaches about $0.025\,\text{W m}^{-2}$ regardless of the model and the frequency. The first row in Fig. 4 clearly shows that sPD on "min" model is larger compared to sPD on both "max" model and a planar surface at $d = 2.5\,\text{mm}$. This difference is the largest at 2.4 GHz where the relative percentage difference, computed as in (6), amounts to 19.53 %. At $d \leq 5\,\text{mm}$, relative differences in sPD between "min" model and both "max" model and a planar surface is positive indicating that sPD on "min" model is larger (substantially at $d = 2\,\text{mm}$ and marginally at $d = 5\,\text{mm}$). However, given the strong curvature of "min" model, by increasing d above 5 mm, relative differences become negative reaching up to 11 % compared to both "max" model and a planar surface. As expected, relative differences between "max" model and a planar surface are negligible since such a large radius results in only slightly curved control surface. Results presented here indicate that strong variations in radii of nonplanar parts on the human head have a substantial effect on sPD reaching up to 25 % larger values compared to the planar model in near field. However the effect is reversed at $d \geq 10\,\text{mm}$ where sPD is up to 12 % less on "min" model compared to the planar model.

IV. Concluding Remarks

In this paper, the EM exposure of human head to the Microsoft HoloLens, a mixed reality smart glasses, was analyzed. For simplicity sake, the Wi-Fi antenna embedded into the HoloLens was modeled as a half-wavelenght dipole operating at 2.4 and 5 GHz. In addition, we simulated exposure to the external antenna at 10 GHz to consider the support of 5G network connection via dongle, but also to justify the choice of the exposure metrics. The (exposure) reference level was determined by means of the spatially averaged IPD on a square $4\,\text{cm}^2$ control surface. A human head was modeled as a regular sphere with varying radius depending on the age of the exposed subject. Stochastic analysis of the influence of the radius, which directly controls the curvature, on the overall spatially averaged IPD was additionally performed. Two subjects were considered for the analysis: the average adult and five-year-old child.

Results indicate that no significant variability in the spatially averaged IPD occurs for neither adult nor child head for radii in the range ± 3 standard deviations from the expected value. A marginal relative difference between spatially averaged IPD exists on the adult and child head model, but this difference fades at $d > 5\,\text{mm}$. However, there is a substantial difference between spatially averaged IPD reaching up to about 9 % and 11 % on the adult head and planar model, and the child head and planar model, respectively.

Additional analysis of the effect of curvature of small body parts is provided for the radius arbitrarily set to 1.8 cm which roughly corresponds to the half the length of the human

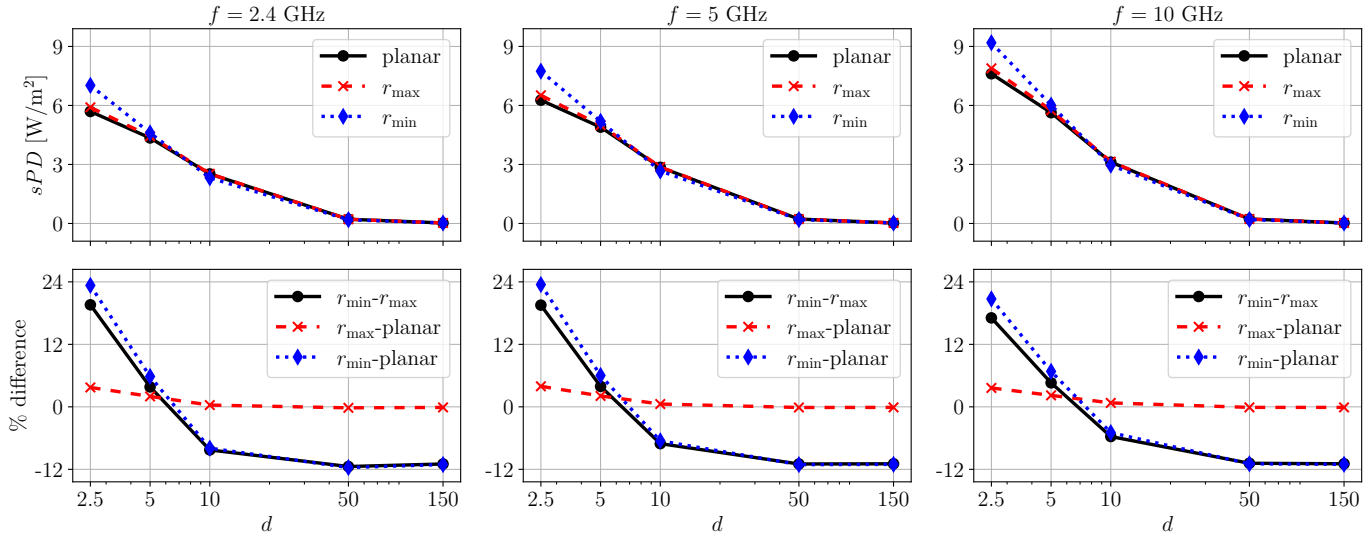

Fig. 4. The first row shows sPD averaged on an evaluation plane (used as a reference) and on the least ($r_{\max}$) and most ($r_{\min}$) curved models as a function of the separation distance from the antenna at 2.4 GHz, 5 GHz and 10 GHz. The second row shows relative differences in sPD between two nonplanar models and between each head model and its planar counterpart.

eyeball. The spatially averaged IPD on the spherical model with aforementioned radius is substantially larger (up to 24 %) compared to the planar and spherical model with tenfold radius. The difference decreases with an increase in d and becomes negative at $d \geq 10\,\mathrm{mm}$ at all considered frequencies. This implies that the separation distance from the antenna strongly affects the spatial distribution of the power density across averaging surface of the small body parts in a relative sense, but in terms of absolute IPD values, the difference is negligible.

Overall results indicate that the curvature effect is an important factor to consider in the future version of guidelines/standards for limiting human exposure to EM fields.

References

[1] J. G. Andrews, S. Buzzi, W. Choi, S. V. Hanly, A. Lozano, A. C. K. Soong, and J. C. Zhang, "What will 5G be?" *IEEE Journal on Selected Areas in Communications*, vol. 32, no. 6, pp. 1065–1082, 2014.

[2] T. S. Rappaport, S. Sun, R. Mayzus, H. Zhao, Y. Azar, K. Wang, G. N. Wong, J. K. Schulz, M. Samimi, and F. Gutierrez, "Millimeter wave mobile communications for 5G cellular: It will work!" *IEEE Access*, vol. 1, pp. 335–349, 2013.

[3] M. T. Specification. (2021) Connect to cellular and 5G. [Online]. Available: https://docs.microsoft.com/en-us/hololens/hololens-cellular

[4] International Commission on Non-Ionizing Radiation Protection (ICNIRP), "Guidelines for limiting exposure to electromagnetic fields (100 kHz to 300 GHz)," *Health Physics*, vol. 118, pp. 483–524, 2020.

[5] "IEEE standard for safety levels with respect to human exposure to electric, magnetic, and electromagnetic fields, 0 Hz to 300 GHz," *IEEE Std C95.1-2019 (Revision of IEEE Std C95.1-2005/ Incorporates IEEE Std C95.1-2019/Cor 1-2019)*, pp. 1–312, 2019.

[6] M. C. Ziskin, S. I. Alekseev, K. R. Foster, and Q. Balzano, "Tissue models for RF exposure evaluation at frequencies above 6 GHz," *Bioelectromagnetics*, vol. 39, no. 3, p. 173–189, 2018.

[7] D. Funahashi, T. Ito, A. Hirata, T. Iyama, and T. Onishi, "Averaging area of incident power density for human exposure from patch antenna arrays," *IEICE Transactions on Electronics*, vol. E101.C, no. 8, pp. 644–646, 2018.

[8] K. R. Foster, M. C. Ziskin, and Q. Balzano, "Thermal response of human skin to microwave energy: a critical review," *Health Physics*, vol. 111, no. 6, pp. 528–541, 2016.

[9] "IEEE guide for the definition of incident power density to correlate surface temperature elevation," *IEEE Std 2889-2021*, pp. 1–152, 2021.

[10] Y. Diao, K. Li, K. Sasaki, S. Kodera, I. Laakso, W. E. Hajj, and A. Hirata, "Effect of incidence angle on the spatial-average of incident power density definition to correlate skin temperature rise for millimeter wave exposures," *IEEE Transactions on Electromagnetic Compatibility*, vol. 63, no. 5, pp. 1709–1716, 2021.

[11] K. Li, Y. Diao, K. Sasaki, A. Prokop, D. Poljak, V. Doric, J. Xi, S. Kodera, A. Hirata, and W. E. Hajj, "Intercomparison of calculated incident power density and temperature rise for exposure from different antennas at 10–90 GHz," *IEEE Access*, vol. 9, pp. 151 654–151 666, 2021.

[12] K. Li, K. Sasaki, K. Wake, T. Onishi, and S. Watanabe, "Quantitative comparison of power densities related to electromagnetic near-field exposures with safety guidelines from 6 to 100 GHz," *IEEE Access*, vol. 9, pp. 115 801–115 812, 2021.

[13] E. Carrasco, D. Colombi, K. R. Foster, M. Ziskin, and Q. Balzano, "Exposure assessment of portable wireless devices above 6 GHz," *Radiation Protection Dosimetry*, vol. 183, no. 4, pp. 489–496, 2018.

[14] G. Sacco, Z. Haider, and M. Zhadobov, "Exposure levels induced in curved body parts at mmWaves," *IEEE Journal of Electromagnetics, RF, and Microwaves in Medicine and Biology*, vol. Early Access, 2022.

[15] M. T. Specification. (2022) Connect HoloLens to a network. [Online]. Available: https://docs.microsoft.com/en-us/hololens/hololens-network

[16] K. Mei, "On the integral equations of thin wire antennas," *IEEE Transactions on Antennas and Propagation*, vol. 13, no. 3, pp. 374–378, 1965.

[17] D. Poljak, *Advanced Modeling in Computational Electromagnetic Compatibility*. John Wiley & Sons, Inc., 2006.

[18] Z. Zhuang, D. Landsittel, S. Benson, R. Roberge, and R. Shaffer, "Facial anthropometric differences among gender, ethnicity, and age groups," *The Annals of Occupational Hygiene*, vol. 54, no. 4, pp. 391–402, 2010.

[19] M. de Onis, A. Onyango, E. Borghi, A. Siyam, and A. Pinol, *WHO Child Growth Standards*. WHO Press, 2009.

[20] A. Lojic Kapetanovic and P. D., "Assessment of incident power density on spherical head model up to 100 GHz," *IEEE Transactions on Electromagnetic Compatibility*, accepted for publishing.

[21] A. Šušnjara, H. Dodig, D. Poljak, and M. Cvetković, "Stochastic-deterministic thermal dosimetry below 6 GHz for 5G mobile communication systems," *IEEE Transactions on Electromagnetic Compatibility*, vol. 63, no. 5, pp. 1667–1679, 2021.